COMMUNICATION

Template-directed conjugation of heterogeneous oligonucleotides to a homobifunctional molecule for programmable supramolecular assembly

Received 00th January 20xx,
Accepted 00th January 20xx

DOI: 10.1039/x0xx00000x

Seham Helmi*[a,b] and Andrew J. Turberfield *[a,b]

Nanoscience aspires to mimic nature's control over functional molecular assemblies. Here we present a templating technique for the efficient attachment of two different oligonucleotides to a homobifunctional molecule, enabling its controlled and programmable placement within a DNA nanostructure. We demonstrate its application to a range of organic molecules with different conjugation chemistries and water solubilities. We show that the two oligonucleotide adapters can be used to integrate a bifunctional cyanine dye into a self-assembled 3D-DNA origami nanostructure, giving control of both position and orientation. We also demonstrate the use of both adapters to exert dynamic control over the environment of the target molecule by means of a series of strand-displacement reactions.

The emerging field of DNA-supramolecular chemistry[1,2] combines the control and programmability of structural DNA nanotechnology[3] with the remarkable capabilities of supramolecular chemistry[4]. It relies on the fabrication of oligonucleotide hybrids, incorporating organic or inorganic building blocks, that can be used to augment the structural motifs of conventional nucleic acid nanostructures[5–13]. Functional molecules conjugated to oligonucleotide adapters can be positioned precisely within self-assembled DNA nanostructures[14–21] to create supramolecular architectures for, for example, nanophotonics[17,18], molecular electronics[19,20], and synthetic enzyme cascades[21,22]. Generally, the heterologous building block can be attached on-column, during solid-support oligonucleotide synthesis[5–10,18], or post-synthetically[11,12]. On-column synthesis, e.g. through phosphoramidite chemistry, requires appropriate protection of reactive groups to prevent off-target reactions. Preparing oligonucleotide conjugates post-synthetically reduces or removes the need for functional group protection and the harsh, basic conditions used for deprotection in phosphoramidite oligonucleotide synthesis. On the other hand, it can be difficult to find a solvent compatible with both the highly-charged oligonucleotide backbone and a relatively hydrophobic molecule.

It may be advantageous to create a hybrid in which a functional building block is inserted within the oligonucleotide backbone rather than appended at a terminus. Oligonucleotide domains on either side provide additional control over the position and orientation of the building block when integrated into a self-assembled DNA or RNA nanostructure. On-column synthesis allows a heterologous moiety to be incorporated after synthesis of the first flanking domain and before the second. Here, we demonstrate a general method for post-synthetic coupling of two oligonucleotides with different base sequences to a homobifunctional molecule in a one-pot reaction.

Our method is developed from Liu's DNA-templated synthesis (DTS)[23] in which reactants are pre-conjugated to oligonucleotide adapters that serve to identify and control their reactions. Hybridization between adapters, or between two adapters and a third "template" oligonucleotide, forces reactants into proximity, increasing the effective local concentration of one at the other and hence selectively increasing their reaction rate[23–31]. The method is illustrated in Figure 1A. A template oligonucleotide hybridizes to the two different adapters which are functionalized with reactive groups complementary to those of the homobifunctional target molecule. The templating DNA complex increases the local concentration of the second adapter's reactive group once the first reaction has occurred. This favours the selective attachment of the target molecule to two adapters with different sequences over side reactions in which two adapters of the same sequence, or only one adapter, are attached.

To test this strategy, we performed copper-catalyzed azide-alkyne cycloaddition (CuAAC) reactions in the presence and absence of the templating oligonucleotide (Figure 1B).

[a] *Department of Physics, University of Oxford, Clarendon Laboratory, Parks Road, Oxford OX1 3PU United Kingdom*
[b] *The Kavli Institute for Nanoscience Discovery, University of Oxford, New Biochemistry Building, South Parks Road, Ox-ford OX1 3QU United Kingdom.*
Email: seham.helmi@physics.ox.ac.uk; andrew.turberfield@physics.ox.ac.uk

Electronic Supplementary Information (ESI) available: Experimental section, Yield calculation, Separate color-channel images for all included gels, HPLC traces, Figures S1–S14, control experiments for Figure 5, origami design. See DOI: 10.1039/x0xx00000x

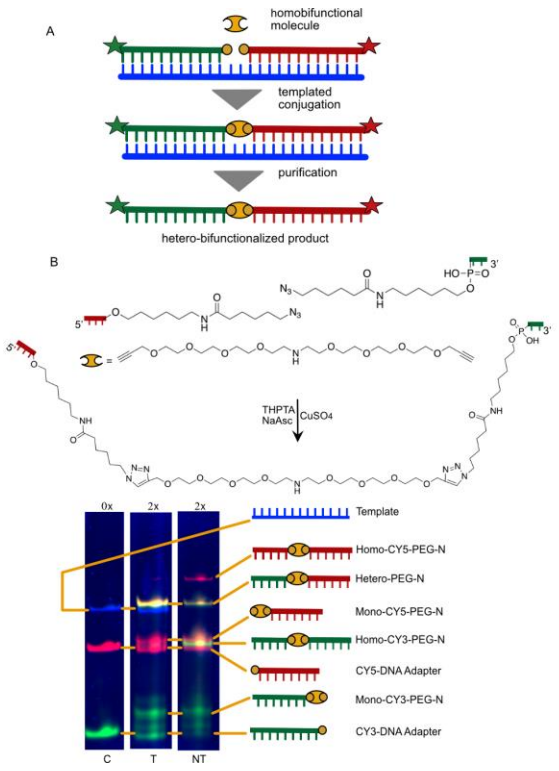

Figure 1. Template-directed conjugation. A) The DNA template (blue) is used to localize, through hybridization, two distinct DNA adapters (red and green) creating a short gap that accommodates the homobifunctional molecule to be conjugated. DNA adapters are identified by Cy3 (green) and Cy5 (red) fluorescent labels, allowing the desired hetero-functionalized product to be readily identified. B) Merged color image of 20% denaturing PAGE gel showing products of templated (T) and non-templated (NT) reactions of alkyne-PEG-N-alkyne with a mixture of two azide-modified DNA adapters. Control (C) contains template and adapters but no target molecule. Cy3 and Cy5 fluorescence channels are green and red respectively; SYBR® Gold DNA stain is blue. Products of the non-templated reaction include all possible hybrids incorporating one or two DNA adapters. The template increases the yield of the hetero-DNA-conjugated molecule (yellow band) and strongly reduces the formation of homobifunctionalized side-products.

The target molecule was a homobifunctional alkyne-modified polyethylene glycol oligomer with a central amine group (PEG-N). To facilitate detection of reaction products the two DNA adapters were labelled with different fluorophores, 3'-Cy3 and 5'-Cy5, at the opposite end to the reactive azide modification.

When the Cy3 and Cy5 adapters hybridize to the template their azide-functionalized termini are separated by a gap of 2 template nucleotides (nt). Reactions in the presence or absence of template were tested with a 2:1:1 ratio of PEG-N to DNA adapters. Full experimental details are provided in the Supporting Information. Reaction products were analysed by denaturing polyacrylamide gel electrophoresis (PAGE): gels were scanned using Cy3, Cy5, and SYBR® gold (DNA stain) fluorescence channels. In the merged gel image (Figure 1B) the yellow band (just above the blue template band) corresponds to colocalized Cy3 and Cy5 fluorescence indicating the desired hetero-DNA-PEG-N product, i.e. PEG-N conjugated to one each of the Cy3- and Cy5-labelled DNA adapters. Yields were estimated from integrated Cy5 and Cy3 fluorescence intensities of the corresponding gel bands. In the presence of the template approximately 58% yield of the hetero-DNA-PEG-N hybrid was obtained (relative to the concentration of either adapter) with barely detectable yield of off-target homo-functionalized PEG-N. Side products are mainly mono-DNA-functionalized PEG-N. In the absence of template the yield of hetero-DNA-PEG-N was approximately 20%, with comparable yields (19% - 24%) of both homo-DNA-PEG-N hybrids. These results confirm that the template is effective in favouring reaction with both co-localized adapters, as designed. The very low yield of homo-DNA-PEG-N hybrids in the templated reaction suggest that the templated complex also discriminates against the formation of homo-DNA-PEG-N hybrids by steric hindrance of the approach of a non-templated oligonucleotide.

To test the extent to which the distribution between reaction products can be biased by templating, we repeated the CuAAC coupling reactions with higher PEG-N concentrations (Figure 2A). The simplest model (independent reactions at either end of the target molecule) predicts that, in the absence of template, the absolute yields of both hetero-DNA and homo-DNA products decrease as the excess of target molecules increases, as the inverse of the molar ratio of target to adapters, with a corresponding increase in the yields of mono-DNA hybrids. Our results in the absence of template are qualitatively consistent with this model (Figure 2C). However, the yield of hetero-DNA-PEG-N decreases more slowly than predicted as the concentration of PEG-N increases; this may reflect a weak

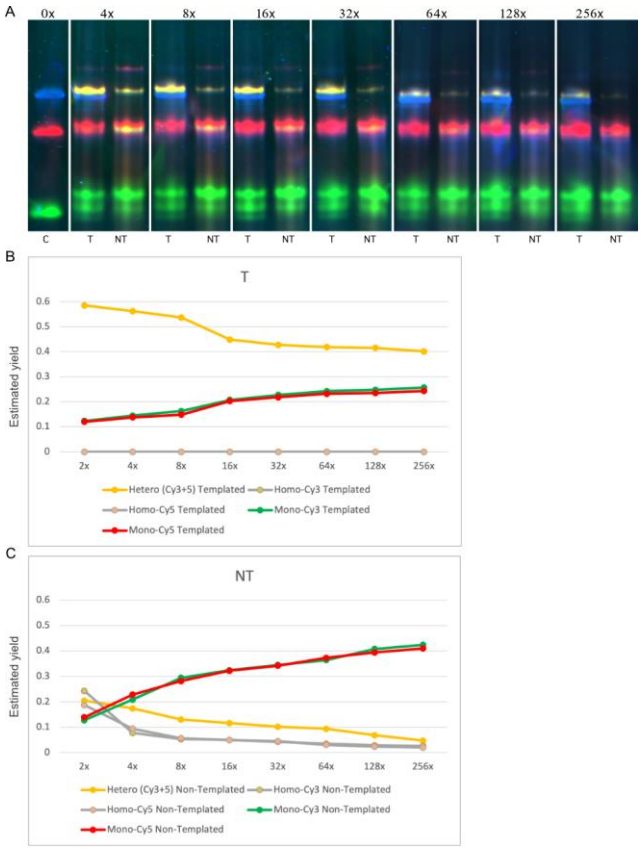

Figure 2. Reaction yields as functions of PEG-N concentration. A) Denaturing PAGE gels showing products of templated (T) and non-templated (NT) CuAAC reactions, as Figure 1B. "n×" indicates the molar excess of PEG-N over adapters (n:1:1). Yellow color in the vicinity of red Cy5 bands corresponds to overlap between them and the green homo-Cy3-PEG-N band (cf. SI- Figure S4), not to a heterofunctionalized product. B&C) normalized yields of (B) templated and (C) non-templated reactions.

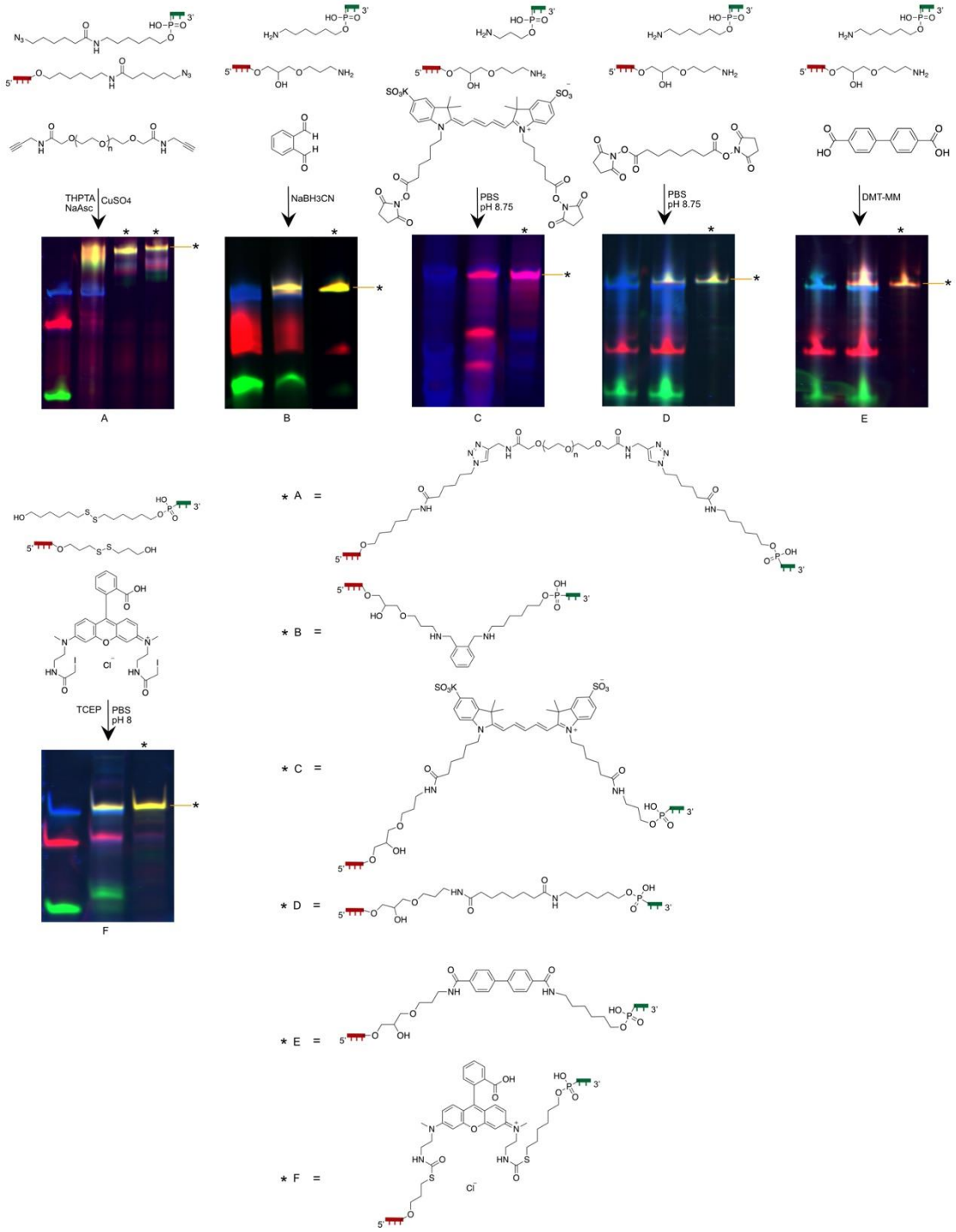

Figure 3. Templated heterofunctionalization of a wide range of targets. A) CuAAC with alkyne-PEG5000-alkyne; B) reductive amination of phthaldialdehyde; C) amide bond formation with sulfo-cyanine 5 bis-NHS ester; D) amide bond formation with DSS linker; E) amide bond formation with biphenyl di-carboxylic acid; F) alkylation of bifunctional rhodamine iodoacetamide. Merged fluorescence images (cf. Figure 1B) are of 20% denaturing PAGE gels comprising: 1st lane, unreacted oligonucleotides; 2nd lane, reaction products; 3rd lane (and 4th lane in gel A), HPLC-purified heterofunctionalized product (marked *). The heterofunctionalized product band (marked —*). In Gel C, Cy5 channel shows the target molecule; adapters were not fluorescently labelled. Template gaps between functionalized adapters were 1 nt (A, B) or 2 nt (C-F).

residual templating effect due to non-designed interactions between DNA adapters. As expected, mono-DNA-PEG-N hybrids were the dominant products in each non-templated reaction. The most important result is that templating greatly increases the yield of the target hetero-DNA-PEG-N hybrid at all concentrations (Figure 2B). The yield of the templated reaction

is only weakly dependent on the excess concentration of PEG-N, decreasing from 58% at 2× to 40% at 256× PEG-N. In fact, the yield of the target product exceeded that of both mono-DNA-PEG hybrids for all excess PEG-N concentrations tested (Figure 2B,C, S1).

To demonstrate the flexibility of the double-templating technique, we applied it to homobifunctional organic molecules with different sizes, water solubilities and conjugation chemistries (Figure 3). Reaction conditions and product purification are described in Supporting Information. Figure 3A shows CuAAC conjugation to a polymer, a homobifunctional alkyne-modified PEG with an average of 5000 ethylene glycol units (PEG5000). The 1-nt template gap between azide-functionalized DNA adapters is three orders of magnitude smaller than the contour length of the polymer. Two products were identified and collected by HPLC (Figure S7). Gel analysis is consistent with the interpretation that both are hetero-DNA-PEG hybrids with an estimated total yield of 97%: we attribute the difference between them to inhomogeneity in the PEG5000 sample.

Figure 3B and 3C show products of coupling, by reductive amination, of amine-modified DNA adapters to phthaldialdehyde and formation of amide bonds to sulfo-cyanine 5 bis-NHS ester, respectively. The template gaps in these cases are similar in size to the target molecule. Estimated yields were 65% and 55%, respectively.

Coupling to water-insoluble molecules is demonstrated in Figures 3D-F, which show DNA-templated formation of amide bonds to disuccinimidyl suberate (DSS) and biphenyl-4,4'-dicarboxylic acid and an alkylation reaction be-tween thiol-functionalized DNA adapters and N,N'-bis[2 (iodoacetamido)ethyl]-N,N'-dimethylrhodamine dihydroiodide. Target molecules were initially dissolved in dimethyl formamide (DMF); reactions took place in mixed aqueous solution comprising 15% DMF. Estimated yields were 31%, 40% and 49%, respectively, with no detectable yield of homobifunctionalized products and traces of monofunctionalized products in the case of rhodamine only.

Conjugation to two different DNA adapters enables integration of a target molecule in a DNA nanostructure[5–7, 14,15,19] with control of both position and orientation. Figure 4 shows integration of hetero-DNA-Cy5 in a three-dimensional DNA origami nanostructure[32]. The DNA adapters of the hetero-DNA-Cy5 hybrid were designed to be complementary to origami scaffold domains flanking a small window in the structure, enabling insertion of the fluorophore within the window through hybridization to the scaffold on either side. Purified hetero-DNA-Cy5 was added either as a staple strand during origami assembly or annealed to a pre-assembled origami. Agarose gel analysis confirmed integration of the Cy5 molecule into the assembled origami in both cases (Figure 4B lanes 3 and 5, respectively).

Figure 5 demonstrates the use of both conjugated adapters to exert dynamic control of the target molecule in a series of strand-displacement reactions[33]. Each reaction, triggered by addition of an oligonucleotide, changes the environment of a hetero-DNA-Cy5 hybrid (Figure 3C*). The second fluorescent component is a singly-DNA-conjugated Cy3. Figure 5B shows fluorescent products after each transition: results are consistent with the reaction scheme. After transitions 2 and 3 the two fluorophores are held in close proximity resulting in Förster resonance energy transfer (FRET) which is identified in measurements of Cy5 fluorescence during excitation of Cy3 only (Figure 5C; a gel image showing the corresponding FRET channel and control experiments are shown in SI).

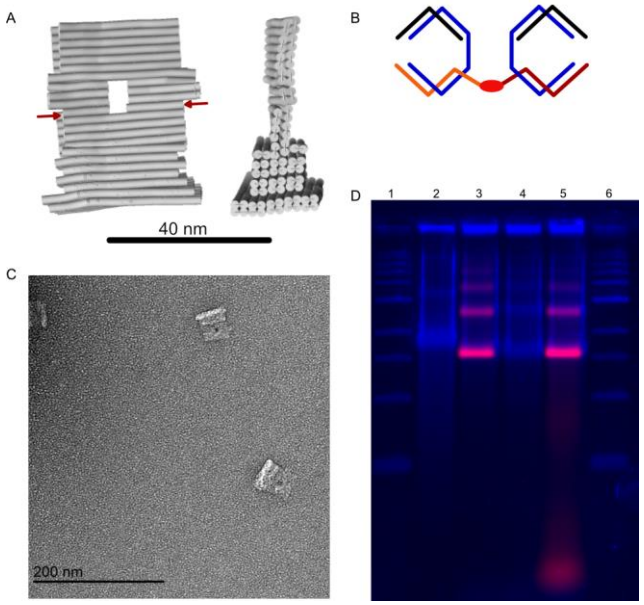

Figure 4. Insertion of a hetero-DNA-Cy5 hybrid in a DNA origami nanostructure. A) CanDo[34] simulation of 3D origami design. Cylinders represent double helices connected by reciprocal staple crossovers. Red arrows indicate the helix into which the Cy5 molecule is to be integrated. B) Schematic showing integration of hetero-DNA-Cy5 hybrid by hybridization of the two DNA adapters (red & orange) to the origami scaffold (blue). C) TEM image of the assembled origami. D) Analysis of origami by 2% agarose gel. Image merges fluorescence from Cy5 (red) and SYBR® Gold DNA stain (blue). Lanes: 1 & 6: 1kb ladder, 2: p8064 scaffold, 3: origami with Cy5 integrated during assembly, 4: origami without Cy5, and 5: origami of lane 4 with Cy5 integrated through post-assembly annealing. The most prominent bands in lanes 3 and 5 displaying Cy5 fluorescence correspond to origamis incorporating the heterofunctionalized dye; fainter red bands are origami multimers.

Conclusions

Our results indicate that the double-templating technique can be applied to a wide range of conjugation reactions and target molecules, including polymers and water-insoluble compounds, while providing high yields of the target hetero-DNA-functionalized hybrids. This efficient, post-synthetic method for the simultaneous attachment of two adapters will be particularly useful where molecular components are incompatible with solid-phase oligonucleotide synthesis. Provision of two different oligonucleotide adapters to control the insertion and alignment of functional molecules in DNA nanostructures increases our control over the assembly of complex supramolecular assemblies. This method will facilitate future applications of DNA nanostructures to control the architectures of multi-component molecular systems such as

multi-enzyme cascades and integrated molecular electronic circuits.

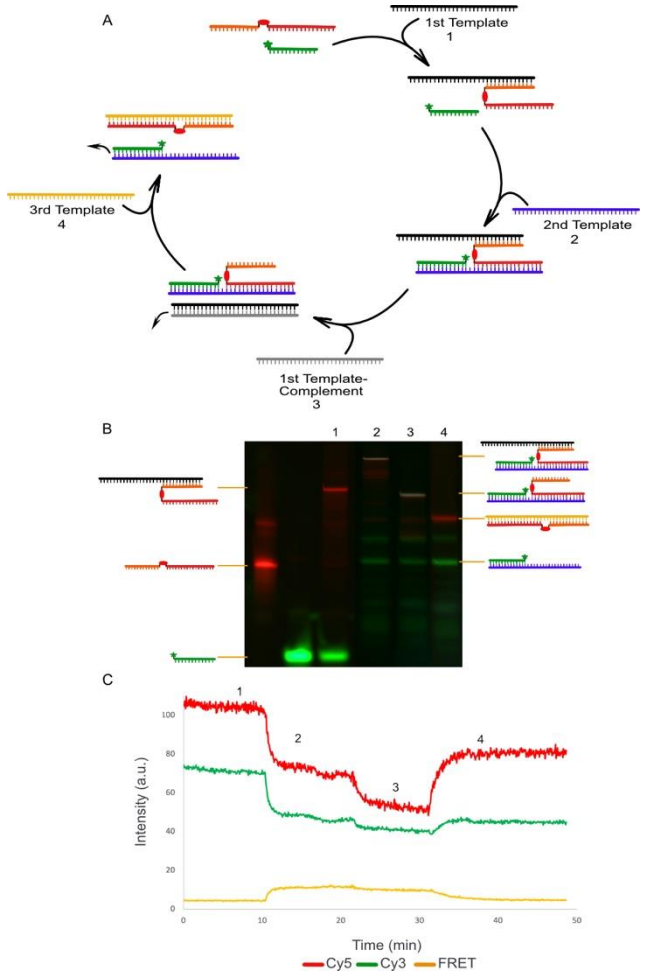

Figure 5. Hybridization reactions demonstrating programmed control of a hetero-DNA-Cy5 hybrid by means of the two oligonucleotide adapters. A) Hybridization reaction sequence. B) 10% native PAGE gel showing reaction products imaged in Cy5 (red) and Cy3 (green) fluorescence channels. Yellow bands correspond to products containing both fluorophores. C) Characterization of reaction progression by fluorescence spectroscopy. The FRET signal corresponds to Cy5 emission under excitation of Cy3. FRET is characteristic of complexes in which Cy3 and Cy5 are held in close proximity.

Conflicts of interest

There are no conflicts to declare.

ACKNOWLEDGMENT

We thank Dr. Jonathan Bath for helpful discussions, Dr. Rana Abdul Razzak for help with manuscript revision and Dr. Deepak Asthana and Prof. Richard E. P. Winpenny for providing the PEG-N molecule. This project was supported by Engineering and Physical Sciences Research Council grant EP/P000479/1.

Notes and references

1 F. A. Aldaye, A. L. Palmer, and H. F. Sleiman. Science, 2008, 321, 1795–1799.
2 C. K. McLaughlin, G. D. Hamblin, and H. F. Sleiman. Chemical Society Reviews, 2011, 40, 5647–5656.
3 N. C. Seeman and H. F. Sleiman. Nature Reviews Materials, 2017, 3.
4 J. M. Lehn. Angew Chem Int Ed Engl, 1988, 6, 89–112.
5 W. Wang, W. Wan, H. H. Zhou, S. Niu, and A. D. Q. Li. Journal of the American Chemical Society, 2003, 125, 5248–5249.
6 F. A. Aldaye, P. K. Lo, P. Karam, C. K. McLaughlin, G. Cosa, and H. F. Sleiman. Nature Nanotechnology, 2009, 4, 349–352.
7 K. v. Gothelf, A. Thomsen, M. Nielsen, E. Ció, and R. S. Brown. Journal of the American Chemical Society, 2004, 126, 1044–1046.
8 T. G. W. Edwardson, K. M. M. Carneiro, C. K. McLaughlin, C. J. Serpell, and H. F. Sleiman. Nature Chemistry, 2013, 5, 868–875.
9 M. S. Shchepinov, K. U. Mir, J. K. Elder, M. D. Frank-Kamenetskii, and E. M. Southern. Nucleic Acids Research, 1999, 27, 3035–3041.
10 M. Scheffler, A. Dorenbeck, and M. Wüstefeld. Angewandte Chemie - International Edition, 1999, 38, 3312–3315.
11 M. F. Jacobsen, J. B. Ravnsbaek, and K. v. Gothelf. Organic and Biomolecular Chemistry, 2010, 8, 50–52.
12 M. Endo, N. C. Seeman, and T. Majima. Angewandte Chemie - International Edition, 2005, 44, 6074–6077.
13 F. A. Aldaye and H. F. Sleiman. Journal of the American Chemical Society, 2007, 129, 13376–13377.
14 F. A. Aldaye and H. F. Sleiman. Angewandte Chemie - International Edition, 2006, 45, 2204–2209.
15 F. A. Aldaye and H. F. Sleiman. Journal of the American Chemical Society, 2007, 129, 4130–4131.
16 K. Tanaka, G. H. Clever, Y. Takezawa, Y. Yamada, C. Kaul, M. Shionoya and T. Carell. Nature Nanotechnology, 2006, 1, 190–194.
17 K. Hübner, M. Pilo-Pais, F. Selbach, T. Liedl, P. Tinnefeld, F. D. Stefani, and G. P. Acuna. Nano Letters, 2019, 19, 6629–6634.
18 M. Madsen, M. R. Bakke, D. A. Gudnason, A. F. Sandahl, R. A. Hansen, J. B. Knudsen, A. L. B. Kodal, V. Birkedal and K. V. Gothelf. ACS Nano, 2021, 15, 9404–9411.
19 X. Wang, R. Sha, M. Kristiansen, C. Hernandez, Y. Hao, C. Mao, J. W. Canary and N. C. Seeman. Angewandte Chemie - International Edition, 2017, 56, 6445–6448.
20 J. B. Knudsen, L. Liu, A. L. B. Kodal, M. Madsen, Q. Li, J. Song, J. B. Woehrstein, S. F. J. Wickham, M. T. Strauss, F. Schueder, J. Vinther, A. Krissanaprasit, D. Gudnason, A. A. A. Smith, R. Ogaki, A. N. Zelikin, F. Besenbacher, V. Birkedal, P. Yin, W. M. Shih, R. Jungmann, M. Dong and K. V. Gothelf. Nature Nanotechnology, 2015, 10, 892–898.
21 J. Fu, M. Liu, Y. Liu, N. W. Woodbury, and H. Yan. Journal of the American Chemical Society, 2012, 134, 5516–5519.
22 J. Fu, Y. R. Yang, S. Dhakal, Z. Zhao, M. Liu, T. Zhang, N. G Walter and H. Yan. Nature Protocols, 2016, 11, 2243–2273.
23 X. Li and D. R. Liu. Angewandte Chemie - International Edition, 2004, 43, 4848–4870.
24 Z. J. Gartner, B. N. Tse, R. Grubina, J. B. Doyon, T. M. Snyder, and D. R. Liu. Science, 2004, 305, 1601–1605.
25 Z. J. Gartner, M. W. Kanan, and D. R. Liu. Journal of the American Chemical Society, 2002, 124, 10304–10306.
26 Z. J. Gartner, M. W. Kanan, and D. R. Liu. Angewandte Chemie - International Edition, 2002, 41, 1796–1800.
27 J. L. Czlapinski and T. L. Sheppard. Journal of the American Chemical Society, vol. 123, no. 35, pp. 8618–8619, 2001.
28 M. L. McKee, P. J. Milnes, J. Bath, E. Stulz, A. J. Turberfield, and R. K. O'Reilly. Angewandte Chemie - International Edition, 2010, 49, 7948–7951.

29 W. Meng, R. A. Muscat, M. L. McKee, P. J. Milnes, A. H. El-Sagheer, J. Bath, B. G. Davis, T. Brown, R. K. O'Reilly and A. J. Turberfield. Nature Chemistry, 2016, 8, 542–548.
30 M. W. Kanan, M. M. Rozenman, K. Sakural, T. M. Snyder, and D. R. Liu. Nature, 2004, 431, 545–549.
31 M. L. McKee, P. J. Milnes, J. Bath, E. Stulz, R. K. O'Reilly, and A. J. Turberfield. Journal of the American Chemical Society, 2012, 134, 1446–1449.
32 S. M. Douglas, H. Dietz, T. Liedl, B. Högberg, F. Graf, and W. M. Shih. Nature, vol. 459, no. 7245, pp. 414–418, May 2009.
33 B. Yurke, A. J. Turberfield, A. P. Mills, F. C. Simmel, and J. L. Neumann. Nature, 2000, 406, 605–608.
34 C. E. Castro, F. Kilchherr, Do-N. Kim, E. L. Shiao, T. Wauer, P. Wortmann, M. Bathe and H. Dietz. Nat. Methods, 2011, 8, 221–229.

